THE ASTROPHYSICAL JOURNAL, 442:794–811, 1995 April 1

THE THRESHOLD FOR STELLAR WINDS IN HOT MAIN-SEQUENCE STARS

JAMES A. GRIGSBY[1]
Department of Physics, Wittenberg University, P.O. Box 720, Springfield, OH 45501
AND
NANCY D. MORRISON[1]
Ritter Astrophysical Research Center, University of Toledo, Toledo, OH 43606
Received 1993 December 2; accepted 1994 September 30

ABSTRACT

The profiles of ultraviolet resonance lines of C IV were surveyed in a sample of 29 cluster and assocation members in the spectral type range O9–B2 III–V, together with a few field stars of interest. The temperatures and gravities of the stars were taken from the model atmosphere analysis by Grigsby, Morrison, & Anderson (1992), and the luminosities were estimated on the basis of cluster and association distances from the recent literature. A parameter P_w, was defined in order to describe the degree of asymmetry of the C IV profile. This parameter, together with total C IV equivalent width, was found to be well correlated with stellar luminosity and temperature. A few anomalous stars were noted: τ Sco, HD 66665, HD 13621, and the ON stars HD12323 and HD 201345. The results suggest a sudden onset of observable mass loss at $T_{\rm eff} = 27{,}500 \pm 500$ K, $\log (L/L_\odot) = 4.4 \pm 0.1$, in agreement with the previous study by Prinja (1989). At $T_{\rm eff} = 28{,}000$ K and $\log g = 4$, our non-LTE model atmospheres show an enhancement in the ground-state population of C^{+3} in their topmost layer, which could be responsible for initiation of the winds via radiation pressure on the C^{+3} ions, or for the onset of visibility of C^{+3} ions in the wind because of an increase in the optical depth in the C IV lines in the outermost layers.

Subject headings: stars: early-type — stars: mass loss — ultraviolet: stars

1. INTRODUCTION

This paper is a survey of ultraviolet resonance line profiles in a sample of main-sequence stars in the spectral range from O9 to B2, which straddles the theoretical limit of stability of these stellar atmospheres against radiation pressure (Abbott 1979). Our purpose in this survey is to determine more precisely the location on the main sequence of this limit and the dependence of the morphology of the C IV resonance line profile on fundamental stellar parameters above this limit.

Previously, most such studies have concentrated on more luminous stars with stronger winds (e.g., Pauldrach et al. 1990). Studies of O stars (Garmany et al. 1981; Garmany & Conti 1984) found that mass-loss rates in these stars depended upon luminosity roughly in the manner predicted by the radiation-driven wind theory (Castor, Abbott, & Klein 1975; Abbott 1982), but with much unaccounted-for scatter. Investigations of the C IV $\lambda\lambda$1548, 1550 resonance lines in B stars (Barker 1984) showed a strong correlation between the C IV line strength and spectral type, with a large scatter at each spectral type; Walborn & Panek (1984) found a similar trend—without the scatter—on the basis of a smaller sample of stars. Finally, some main-sequence stars have been identified by Walborn, Nichols-Bohlin, & Panek (1985) as having enhanced winds for their spectral types.

More recently, the behavior of wind signatures in this range of spectral types and luminosity classes has been studied by Grady, Bjorkman, & Snow (1987), Howarth & Prinja (1989), and Prinja (1989). Our study differs from theirs in at least two ways. First, all of them studied the wind diagnostics as a function of spectral type, or else in terms of a temperature scale that is calibrated in terms of spectral type, leaving open the possibility that some of the observational scatter that they found is due to errors or to the binning effects in spectral classification. In contrast, we have studied the mass-loss signatures of our sample of stars as a function of effective temperature and gravity. In addition, our non-LTE, line-blanketed model atmospheres provide more insight into the physical conditions in the photosphere underlying the wind. Second, they studied a larger range of spectral type and/or luminosity class. Here we have used a sample of main-sequence stars that covers the region in the H-R diagram around the static limit at least as densely as the samples used in those investigations.

This is the second of two papers on late O and early B-type stars near the main sequence. In the first paper (Grigsby, Morrison, & Anderson 1992, hereafter Paper I) we reported on the analysis of a sample of stars with a line-blanketed, non-LTE model atmosphere code (PAM). In that analysis we derived effective temperatures, surface gravities, and projected rotational velocities from hydrogen and neutral helium lines, and we studied the behavior of the equivalent widths of N II, N III, C II and C III lines as a function of effective temperature in a search for abundance differences from star to star.

In the present paper, we examine the morphology of wind-sensitive ultraviolet resonance lines—N V $\lambda\lambda$1239, 1243, Si IV $\lambda\lambda$1394, 1403, and C IV $\lambda\lambda$1548, 1550—and we conclude that the best probe of onset of the stellar winds is the C IV doublet. We define the "wind parameter" P_w, which measures the asymmetry of this doublet, and we discuss its dependence and that of C IV total equivalent width on stellar temperature, gravity, and luminosity.

Of course, it is conceivable that some stars have winds that are too transparent to be observed even in this sensitive spectral diagnostic, and it is widely recognized that some of the material in the wind is likely unobservable in any case because

[1] Guest Observer with the *IUE* satellite, which is operated jointly by NASA, ESA, and the SERC.

it is ionized by shocks to states higher than C^{+3}. A good discussion of the relevant literature on this point is given by Prinja, Barlow, & Howarth (1990). In hot stars, X-ray emission is thought to be produced in shocks that are created by instabilities in radiation-driven winds (e.g., MacFarlane & Cassinelli 1989), and this emission may be an even more sensitive diagnostic of mass loss. Recently, X-ray surveys of main-sequence stars (Cassinelli et al. 1994; Meurs et al. 1992) have shown that X-ray emission persists farther down the main sequence than does asymmetric C IV absorption. The available evidence is not, however, sufficient to indicate precisely how much farther in terms of effective temperature. One goal of this investigation is to locate more precisely the threshold in the theoretical H-R diagram where stellar winds first appear in the C IV doublet and to identify a mechanism that could cause either the initiation of the wind itself or the development of sufficient optical depth in the wind to cause asymmetric C IV absorption.

In the following, § 2 describes the observational material, § 3 discusses the stars' luminosities and, thence, locations in the H-R diagram, and § 4 discusses the S IV and N V lines. In § 5, we describe our efforts to disentangle the effects of blends on the C IV line profiles, we define the wind parameter, and we discuss its dependence and that of C IV equivalent width on stellar temperature and luminosity. Section 6 discusses C IV line formation in our static, non-LTE, line-blanketed model atmospheres, and § 7 is a discussion of the initiation of winds in light of our results and those of recent X-ray observations of hot stars. Section 8 presents our conclusions.

2. OBSERVATIONAL MATERIAL

The program stars are described more fully in Paper I, along with their selection criteria. Cluster membership and other information may be found in Table 1 of Paper I. The star HD 143275 (δ Sco) was included, even though it has not been carefully checked for photometric constancy, because its angular diameter is known; the star HD 66665, though not a cluster or association member, was included because Massa (1985) has identified that star as one with unusually strong C IV resonance lines. Some OBCN stars have also been included in violation of the same requirements because of their abundance anomalies (Walborn 1976).

Table 1 of the present paper lists the stars from Paper I for which *IUE* observations exist. The data were processed with the standard procedures (Turnrose & Thompson 1984). Observations made by us were processed immediately; the remaining images, which were taken from the *IUE* archives, were processed in early 1987 with the then-current software. All the spectra are well exposed in the region of the C IV doublet, $\lambda\lambda$1548, 1550, but the spectra of the more highly reddened stars tend to be less well exposed at shorter wavelengths. Thus, the data quality is typical of *IUE* spectra, with signal-to-noise ratio similar to that estimated for individual images by Leckrone & Adelman (1989). The unsmoothed spectra have the nominal spectral resolution (Grady & Imhoff 1985). The data were continuum normalized using the routine IUESPEC, developed by the *IUE* Regional Data Analysis Facility (RDAF) staff at Goddard Space Flight Center (IUE

TABLE 1

LUMINOSITIES OF THE PROGRAM STARS

Star (HD/HDE)	Spectral Type	SWP	Association Subgroup/Cluster	Reference	5 log r − 5	Δ(5 log r − 5)	log ($L_*/L_\odot$)	Δ log ($L_*/L_\odot$)
12323.....	ON9.5 V	9652	Per OB1	1	11.8	0.5	4.390	0.20
13621.....	B0.5 IV	30483	Per OB1	1	11.8	0.5	4.896	0.20
21856.....	B1 V	20970	Per OB2	2	7.5	0.2	3.760	0.13
24131.....	B1 V	20845	Per OB2	2	7.5	0.2	3.870	0.13
34816.....	B0.5 V	26726	Ori OB1	3	7.9	0.6	4.450	0.26
35299.....	B1.5 V	18005	Ori OB1a	3	7.9	0.5	3.780	0.22
35653.....	B0.5 V	30479	Aur OB1	4	10.5	0.4	4.578	0.14
36430.....	B2 V	29158	Ori OB1c	3	7.9	0.6	3.430	0.26
36822.....	B0 IV–V	29099	Cr 69	5	8.0	0.2	4.540	0.16
36824.....	B2 V	29165	Ori OB1a	3	7.9	0.5	3.260	0.22
37209.....	B1 V	29160	Ori OB1c	3	7.9	0.6	3.786	0.26
37366.....	O9.5 V	30480	Aur OB1	4	10.5	0.4	4.650	0.14
120307.....	B2 IV	36482	Upper Cen	6	5.7	0.3	3.780	0.19
132058.....	B2 III	17458	Upper Cen	6	5.7	0.3	4.030	0.19
142669.....	B2 IV–V	22091	Upper Sco	6	6.0	0.3	3.620	0.16
142375.....	B0.3 IV	17395	Upper Sco	6	6.0	0.3	4.590	0.15
144470.....	B1 V	13609	Upper Sco	6	6.0	0.3	3.960	0.15
148703.....	B2 III	29161	Upper Sco	6	6.0	0.3	3.610	0.19
149438.....	B0 V	13793	Upper Sco	6	6.0	0.3	4.390	0.16
151985.....	B2 IV	5879	Upper Sco	6	6.0	0.3	3.750	0.16
152246.....	O9 III	16214	Sco OB1	7	11.5	0.3	5.410	0.14
163892.....	O9 IV	29157	Sgr OB1	8	11.3	0.1	5.160	0.13
207538.....	B0 V	8992	Cep OB2	1	9.9	0.3	4.850	0.17
208440.....	B1 V	30482	NGC 7160	1	9.9	0.3	4.070	0.19
214680.....	O9 V	6784	Lac OB1	1	8.5	0.5	4.640	0.21
217101.....	B2 IV–V	18309	Lac OB1	1	8.5	0.3	3.830	0.21
218195.....	O9 III	26975	Cep OB1	1	11.8	0.3	5.370	0.25
218342.....	B0 IV	29164	Cep OB3	1	9.3	0.3	4.680	0.16
251847.....	B1 IV	30481	Gem OB1	9	11.8	0.1	4.570	0.15

REFERENCES.—(1) Garmany & Stencel 1992. (2) Strom, Strom, & Carrasco 1974; IC 348. (3) Anthony-Twarong 1982. (4) Kimeswenger & Weinberger 1989; NGC 1960. (5) Murdin & Penston 1977. (6) Jones 1971, averages quoted in de Geus et al. 1989. (7) Perry et al. 1991. (8) McCall, Richer, & Visvanathan 1990; NGC 6523. (9) Chavarria-K., de Lara, & Hasse 1987; S252/NGC 2175.

RDAF User's Tutorial Manual 1990). This software performs ripple corrections (Barker 1984) automatically and allows the user to view and normalize large segments of spectra. The spectra were normalized by fitting straight line segments to high points across regions several hundred angstroms wide and were smoothed with a five-point boxcar smoothing procedure. The continua produced in this manner by several independent but experienced users of the software are generally astronomer independent to within a few percent and agree well with the predictions (Grigsby 1991; see also Figures 5*a* and 5*b* of this paper) by the non-LTE, line-blanketed model atmosphere code described in Paper I.

3. THE PROGRAM STARS IN THR H-R DIAGRAM

Table 1 lists the luminosities of the cluster and association members and the estimated uncertainties in the luminosity. The $B-V$ colors were taken from Humphreys (1979), Bertiau (1958), and the photometric references found in Table 1 of Paper I. The intrinsic colors used were those of Johnson (1966), and A_v was computed with R_v [the ratio of the total absorption in the V band to the color excess $E(B-V)$] equal to 3.1, following the standard reddening law. Bolometric corrections were taken from Buser & Kurucz (1978), who obtained them by fitting model (LTE) stellar atmospheres to observed fluxes in main-sequence B stars. We have adopted the additive correction of 0.1 to all the bolometric corrections that those authors recommend.

We searched the literature for the best available information on the distance moduli of OB associations, and the results are incorporated into Table 1. For the Sco-Cen association, the subgroup assignments are taken from de Geus, de Zeeuw, & Lub (1989), and for Ori OB1 from Warren & Hesser (1978). For distance moduli, we adopted values from the recent review by Garmany & Stencel (1992), the reanalysis of Ori OB1 by Anthony-Twarog (1982), and the reanalysis of Sco OB1 by Perry, Hill, & Christodoulou (1991). For associations not included in those references, we could find no recent estimate of the distance to the association as a whole. Therefore, we used the best available estimate of the distance modulus of the open cluster belonging to each association. In those cases, the cluster is named in the list of references to Table 1. For some clusters, such as NGC 2175, the distance moduli in the literature differ by as much as 1 mag. In these cases, we chose the estimate that we judged to be based on the soundest methodology and/or the largest number of cluster members.

The uncertainties in luminosity were computed from the sum, in quadrature, of the uncertainties of the quantities that constitute the bolometric magnitude: the bolometric correction, m_v, A_v, and the distance modulus. The estimated errors in these quantities, except for the distance moduli, are upper limits. For the errors in the distance moduli, either we used the uncertainty quoted by the original investigator, or, if no error was quoted, we estimated the uncertainty from the scatter of the main-sequence stars in the cluster H-R diagram. In addition, we estimated the uncertainty in the distance modulus that is due to the radial extent of the cluster or association by assuming that the object in question is spherical with a radius computed from the angular diameter and distance. These errors in the distance modulus are lower limits in that they include only the front-to-back uncertainty in a given cluster (association) due to its finite size, but *not* any systematic errors that may be present. In modern estimates of distance moduli, the formal error in the mean distance modulus is often smaller than the standard error of the individual stars' moduli about the mean, which may indeed, therefore, be dominated by front-to-back scatter in the stellar distances. In our analysis, we took the uncertainty in the distance modulus of a star to be the error quoted for the association or the front-to-back uncertainty, whichever is larger. The uncertainty in A_v results from errors in R_v and the color excess $E(B-V)$. We took the uncertainty in R_v to be 0.2 and the relative uncertainty in $E(B-V)$ to be 15%, an extreme upper limit. Finally, we took the uncertainty in the apparent visual magnitude to be 0.05 and that of the bolometric corrections to be 0.2; both are conservative upper limits. Even with these upper limits, the uncertainties in the luminosities in Table 1 are generally dominated by the uncertainties in the distance moduli, except for stars that are heavily reddened ($A_v > 0.7$), in which case the error in A_v is comparable to or larger than that in the distance modulus.

For binaries in which the V magnitudes of the secondary components are known and in which the separations are less than 10″, we corrected the combined V magnitude to that of the primary alone. For larger separations, we assumed that the published V magnitude refers to the primary alone, and we made no correction. Thus, small corrections were needed for HD 13621 and HD 37209, for which we obtained the magnitudes and separations from the HIPPARCOS Input Catalog (1992). For HD 143275 (δ Sco), we corrected for the companion at $\Delta m = 1.5$ observed by Bedding (1993).

The H-R diagram is shown in Figure 1. Included are the theoretical zero-age main sequence (ZAMS) (*solid line*) and the 5×10^6 year isochrone (*dash-dotted line*) from Maeder & Meynet (1988). Since this age is typical of our program stars, their location just to the right of this isochrone is well explained by stellar evolution. Also included in the figure is the main-sequence boundary at the low-temperature extreme given in Maeder & Meynet (1988). Although our sample of stars was not chosen with the goal of testing the boundaries of the main-sequence band in mind, the sample is indeed confined to the theoretical main sequence.

An examination of the surface gravities derived in Paper I reveals some minor discrepancies. For example, at an effective temperature of 28,000 K, the lower gravity star HD 36822 apparently has a lower luminosity than HD 13621; at $T_{\rm eff} =$ 22,000 K, HD 217101 ($\log g = 4.2$) apparently has a higher luminosity than several stars with significantly lower gravity. However, these discrepancies are all easily accounted for by the uncertainties in the luminosities, and none is significant.

4. EVIDENCE FOR WINDS IN THE N v AND Si IV LINES

Walborn et al. (1985) discuss this topic and display data for some of the stars in the present sample. They find evidence for winds in the N v $\lambda\lambda$1239, 1243 resonance lines in the so-called nitrogen-enhanced stars HD 12323 and HD 201345, and in τ Sco, which they label as peculiar. These authors also suggest that the Si IV resonance lines in τ Sco display weak evidence for a wind through their slight asymmetry.

Figures 2*a* and 2*b* illustrate the evidence for winds in the N v resonance doublet in selected stars in the present sample. The stars HD 218195 and HD 163892 may also show evidence for a wind in N v, but both spectra are extremely noisy due to having been exposed incorrectly and have been omitted. In this group, the lines in HD 12323 and HD 201345 are not asymmetric, but are strong and shortward shifted. The lines in HD 214680 are weak, and any asymmetry seen may be the result of blends—the same is true of HD 37366 and HD 218342 (not

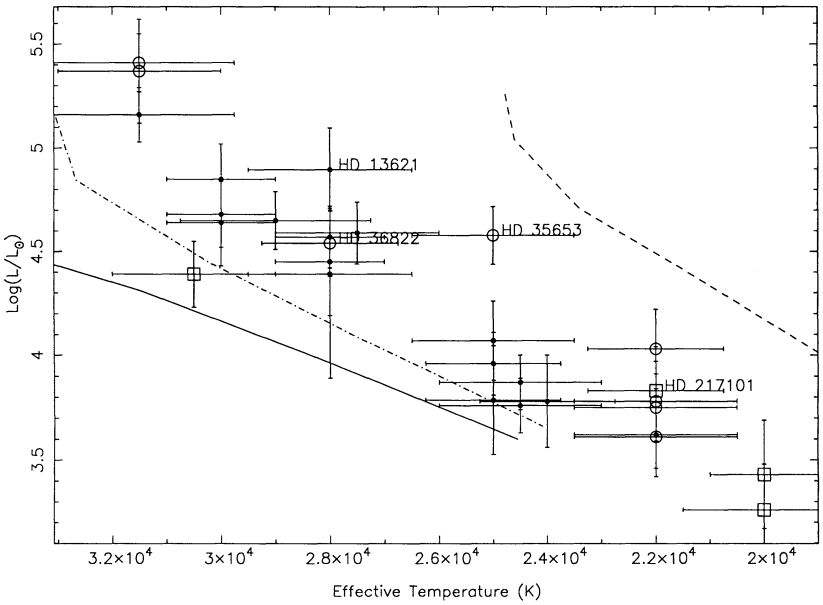

FIG. 1.—H-R diagram of the program stars. The lines are from Maeder & Meynet (1988). The solid line is the theoretical ZAMS. The dash-dotted line is the 5×10^6 yr isochrone, and the dashed line is the low-temperature boundary of the main sequence. Open circles refer to stars with $\log g \leq 3.8$; solid dots, $\log g = 4.0$; open squares, $\log g > 4.0$.

shown). In HD 152246 we see evidence of a broad, shortward-shifted absorption trough, with evidence of P Cygni–type emission, though the noisiness of the spectrum makes the latter conclusion uncertain. In the present sample, the most striking N V lines remain those of τ Sco, but HD 66665 emerges as a close second. Its N V lines are stronger and more asymmetric than those of HD 12323, HD 201345, and HD 214680, even though all of the latter stars have higher effective temperatures according to Paper I. In general, HD 66665 displays unusually strong resonance lines, as shown below and in Grigsby (1992). No longer should τ Sco be viewed as unique for its spectral type (Walborn et al. 1985).

Figures 3*a* and 3*b* show stars that exhibit asymmetries in their Si IV resonance lines. The most pronounced asymmetries occur in HD 66665, HD 152246, and τ Sco. The asymmetry that appears in HD 207538 and HD 218342 may be due to a blend in the wing of the shortward component. The longward component is contaminated by a reseau. Once again, HD 66665 stands out: among the program stars, it has by far the strongest and most asymmetrical Si IV doublet.

Clearly, evidence for winds does occur in the N V and Si IV doublets in some of the program stars. Nevertheless, these lines are difficult to use in the study of wind development because of the weakness of the lines themselves, the weakness of the wind signature, or both. Part of this problem is the nature of the lines and the location (in temperature) of the H-R diagram where the winds switch on: the ionization balance is only beginning to switch to N V in the hottest of the program stars. Conversely, the ionization balance is shifting away from S IV in those stars. The weak dependence of the equivalent width of the Si IV doublet on effective temperature (Grigsby 1992) indicates that this doublet may be an unwise choice for the study of weak winds, at least as a means to test the winds' temperature sensitivity. However, it is the weakness of the wind signatures in these lines that makes them unsuitable. For the study of weak winds, the C IV resonance lines are clearly the best choice.

5. C IV MORPHOLOGY IN THE PROGRAM STARS

5.1. *Contribution of* Fe *Blends in the* C IV *Region*

Hubeny, Stefle, & Harmanec (1985a, b) and Barbier & Swings (1979) have suggested that, in marginal cases, Fe blends in the region of the C IV resonance lines may mimic mass loss. Because we are interested in determining the precise temperature on the main sequence where stellar winds first produce asymmetries in the C IV profiles, we attempted to take blends quantitatively into account. As a first step toward this goal, we calculated synthetic spectra with PAM, which does not include winds, hoping that a close match between the synthetic and the observed spectrum would allow us to decide which features are blends and which are due to wind-enhanced C IV. Figure 4 shows the synthetic spectrum produced by PAM superimposed upon the observed spectrum of HD 37209 ($T_{\rm eff} = 25{,}000$ K, $\log g = 4.0$; Paper I), a spectrum that appears to be affected by photospheric blends only, not by a wind. The synthetic spectrum was calculated by the methods described in Paper I, except that all available opacity sources in the 1525–1560 Å interval (from Kurucz 1987) were included in the solution of the equation of radiative transfer (Grigsby 1991). The available opacity sources in the case of iron include only lines of Fe II and Fe III. The resolutions of the synthetic and observed spectra are identical. The synthetic spectrum has been instrumentally broadened with a Gaussian profile with an FWHM of 0.13 Å to simulate *IUE* instrumental broadening (Grady & Imhoff 1985). It has also been rotationally broadened with a Doppler profile corresponding to a projected rotational velocity of 50 km s^{-1} (Paper I).

It is clear that the model matches many of the features (primarily Fe III) in the region only marginally at best. Many of the lines in the Kurucz data possess incorrect wavelengths, and many are in error in oscillator strength as well. The "lines" (actually, these features are composed of hundreds of individual lines) that are reproduced best are those between 1530 and

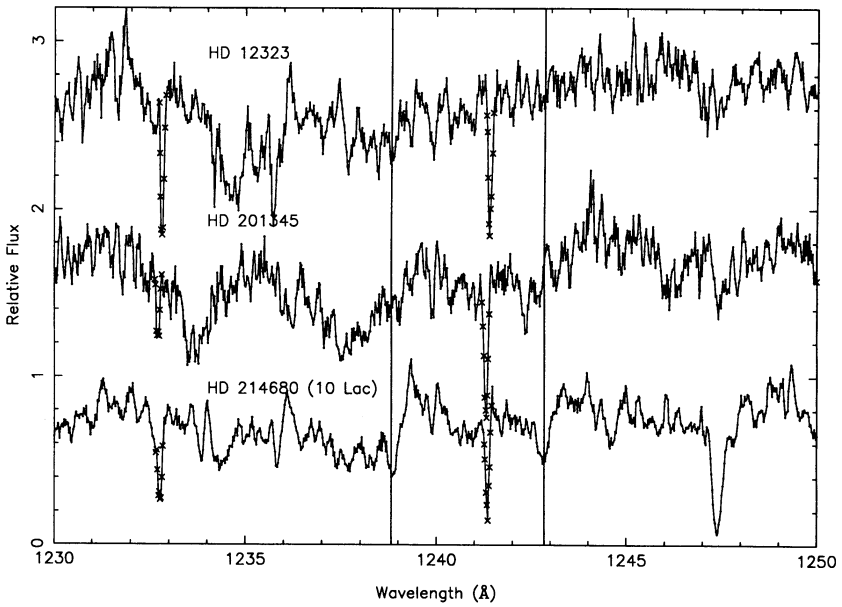

FIG. 2*a*

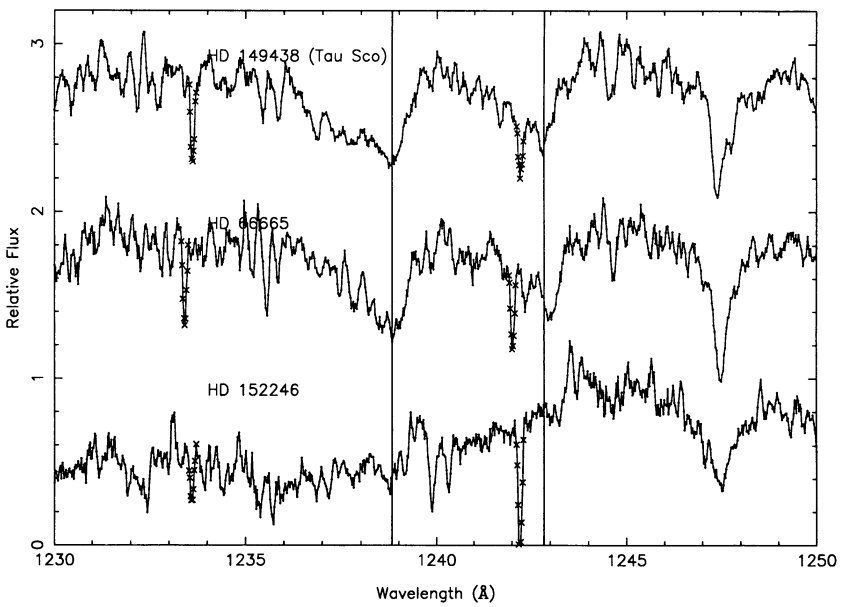

FIG. 2*b*

FIG. 2.—Evidence for winds in the N v doublet for selected stars. In HD 152246 (O9 III), the absorption appears shallow and broad extends off the scale of the graph. There is the possibility of emission at 1243.5 Å. Note the similarity of the profiles in τ Sco and HD 66665 (B0.5 IV). In all cases the HD number of the star appears directly above its spectrum, and the spectra are shifted vertically by an additive constant. Reseaux and other band data flagged by the *IUE* software are indicated by X's. The vertical lines indicate the rest wavelengths of the N v doublet. The apparent redshift of the λ1242.8 line is unexplained. The star's radial velocity of 20 km s^{-1} does not account for it.

1535 Å. The C IV doublet is matched reasonably well, and the blends atop the carbon lines also appear in the model but are too strong. At 1546.5 Å, a line clearly appears in the observation which is not predicted by the model. A search of the Abbott (1985a) line lists reveals a C III line at this wavelength; the same line does not appear in the Kurucz data. It also appears in other stars in the sample, such as HD 24131 ($T_{\rm eff}$ = 24,500 K, log g = 4.0).

If this feature is a line of C III, then it might be expected to increase in strength to a maximum at an effective temperature of ~28,000 K (see Fig. 11 of Paper I) and so may be expected to contribute to the asymmetry that we might otherwise have attributed to the beginnings of a wind in stars such as HDE 251847 ($T_{\rm eff}$ = 28,000 K, log g = 4.0). Figure 5*b* shows what might be interpreted as a strengthened line of C III. However, if that is the case then the line is redshifted by 0.5 Å and asymmetric in the *redward* direction. It is more likely that the line seen in HD 37209 ($T_{\rm eff}$ = 25,000 K, log g = 4.0) is also seen in

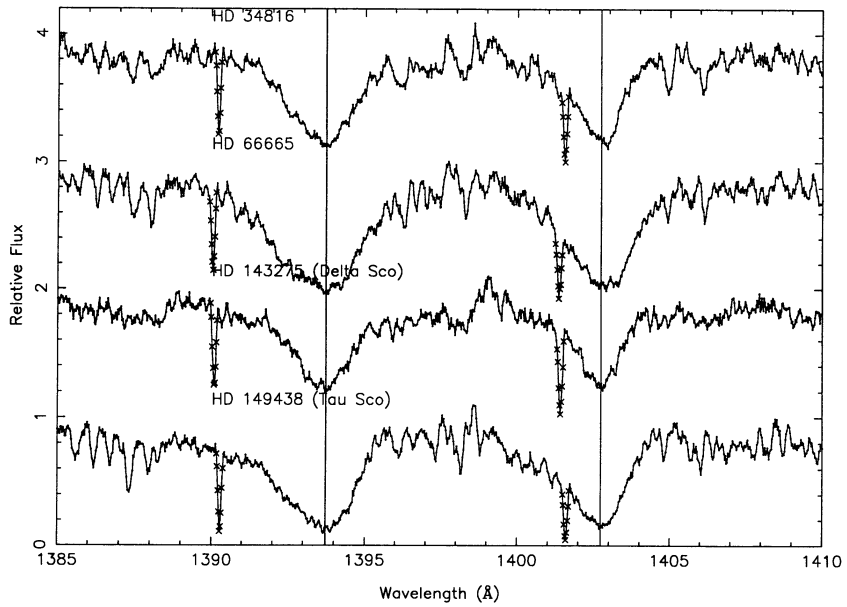

FIG. 3*a*

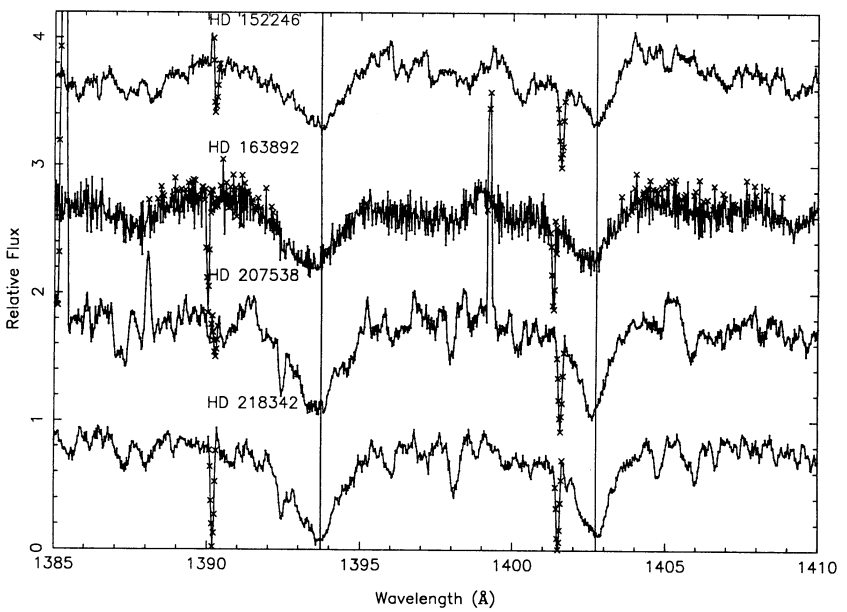

FIG. 3*b*

FIG. 3.—Evidence for winds in the Si IV resonance doublet in selected stars. Note the great strength of these lines in HD 66665 (B0.5 IV). Vertical lines again indicate the position of the rest wavelengths of the doublet.

HDE 251847 at the same wavelength (1545.6 Å). This weaker blend does contribute somewhat to the asymmetric appearance of the line, but the main contributor to the asymmetry seems more likely to be a blueshifted C IV line. At any rate, the blend cannot account for the asymmetry in the longward component of the C IV doublet.

As a final test of the possibility that iron lines may help mimic mass loss, we examine the temperature dependence of the blends (Figs. 5*a* and 5*b*). Published spectra of stars in this temperature range (Rountree & Sonneborn 1991; Walborn et al. 1985) show that the strengths of the blending lines in this spectral range vary little with temperature. On the other hand, in order to mimic the broadening effect of a stellar wind, a blending line must be strongly temperature dependent in the temperature range around 28,000 K. Therefore, it is unlikely that these numerous Fe lines contribute to this effect. To show this point more clearly, in Figures 5*a* and 5*b* we compare the C IV region in HD 66665 ($T_{\rm eff}$ = 28,000 K, log g = 4.0) and HDE 251847 with that in HD 35299 ($T_{\rm eff}$ = 24,000 K, log g = 4.0), all stars with relatively low ($\leq$20 km s^{-1}) projected rotational velocities. Since most of the blends here are due to Fe III (with the exception discussed above), one would expect

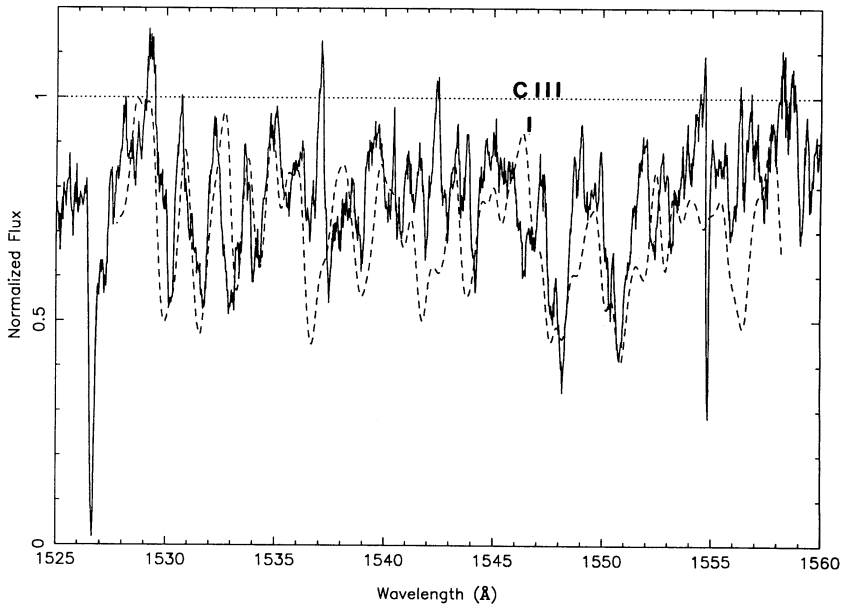

FIG. 4.—Comparison of the observed spectrum of HD 37209 (*solid line*) with the synthetic iron lines and C IV doublet from the model ($T_{\rm eff}$ = 25,000 K, log g = 4.0) presented by Grigsby et al. (1992) (*dashed line*).

that a strong temperature dependence in the lines immediately bordering the C IV doublet would be mimicked by similar behavior in nearby Fe III lines if the shape of the C IV doublet were due to iron blending. Clearly, the lines in the 1540–1545 Å region are not affected much by the increase in temperature, while the C IV doublet is clearly increasing in strength. Indeed, the Fe III lines in HDE 251847 appear to get stronger with the change in temperature than those in HD 66665, while the C IV doublet is clearly weaker in the former star. Fe III lines in the 1520–1540 Å region show behavior similar to those in the figures.

It is clear from the foregoing discussion that the effect seen in the C IV lines is not likely to be due to blending due to iron or carbon. The most straightforward explanation is that most of the asymmetry at 28,000 K is due to a weak wind.

5.2. *Wind Parameter*

The C IV $\lambda\lambda$1548, 1550 resonance doublet is the most sensitive measure of mass loss in the program stars. Since these stars have weak winds, the classical P Cygni profile is not developed, and the wind is revealed primarily through the blueward asymmetry of the C IV resonance lines. Although actual measurements of mass-loss rates would be extremely useful in understanding the mechanisms which initiate winds, we have concluded that we do not have a reliable means of measuring the rates. The approach outlined by Olson (1982) does not work for our stars because evidence for winds typically occurs only in C IV. Alternatively, we could estimate the mass-loss rate from the C IV doublet if the wind's carbon ionization balance were known. With respect to this approach, Lamers & Groenewegen (1990) give empirically derived ionization ratios for C III and C IV at half the wind terminal velocity in giants and supergiants, but not for main-sequence stars in our temperature regime. Therefore, in this paper we do not attempt to derive mass-loss rates, but rather characterize the wind-sensitive feature with a model-independent parameter, which we then examine as a function of the known physical properties of the program stars.

Figures 6*a*–6*c* show the C IV $\lambda\lambda$1548, 1550 resonance doublet in three of the program stars. These spectra illustrate the progression of the strength and asymmetry in what seems to be a fairly smooth sequence. In order to investigate C IV morphology in the program stars we defined a parameter P_w that we term the "wind parameter," as follows:

$$P_w = (\Delta\lambda_b - \Delta\lambda_r)d\ , \qquad (1)$$

where d is the maximum depth of the profile relative to the continuum and where $\Delta\lambda_b$ and $\Delta\lambda_r$ defined as follows:

$$\Delta\lambda_b = \lambda_b - \lambda_b^0 \quad \text{and} \quad \Delta\lambda_r = \lambda_r^0 - \lambda_r\ .$$

Here, λ_b is the wavelength at which the shortward component of the doublet intersects the continuum, and λ_b^0 is the rest wavelength of the shortward component. Similarly, λ_r is the wavelength at which the longward component intersects the continuum and λ_r^0 is that component's rest wavelength. Note that it is possible for $\Delta\lambda_r$ to be negative if the Doppler shift of the doublet is sufficiently large. As an example, Figure 7 illustrates the quantities $\Delta\lambda_b$ and $\Delta\lambda_r$ in the star HD 207538. These definitions ensure that P_w is a measure of the asymmetry and the depth of the profile.

Since blends with weak photospheric lines blur the point at which a typical wind-sensitive profile intersects the continuum, it was necessary to estimate the intersection points. We accomplished this by drawing a profile by hand and extrapolating the observed profile to the continuum where necessary. In stars with low ($\leq$50 km s^{-1}) projected rotational velocities, the extrapolation was minimal. As an example, Figure 7 shows the hand-drawn profile for the star HD 207538. The circles show the points used to define the profile and the point where the hand-drawn profile intersects the continuum. One may argue that the hand-drawn profile may bend over and intersect the continuum at a slightly shorter wavelength; we have chosen the profile that is shown because P Cygni profiles generally exhibit sharp shortward edges (Prinja et al. 1990). Clearly, some ambiguity in the location of the intersection of the profile with the continuum remains, and we have attempted to take

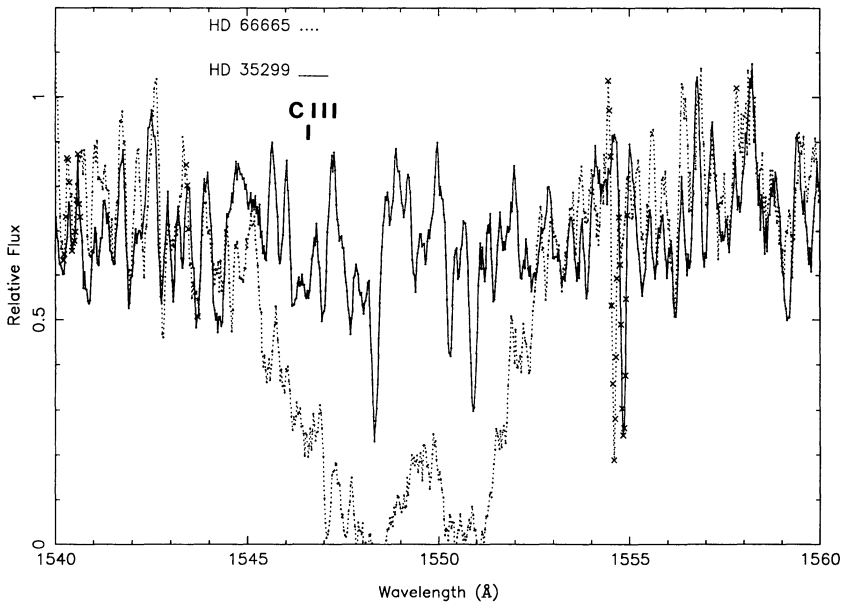

FIG. 5*a*

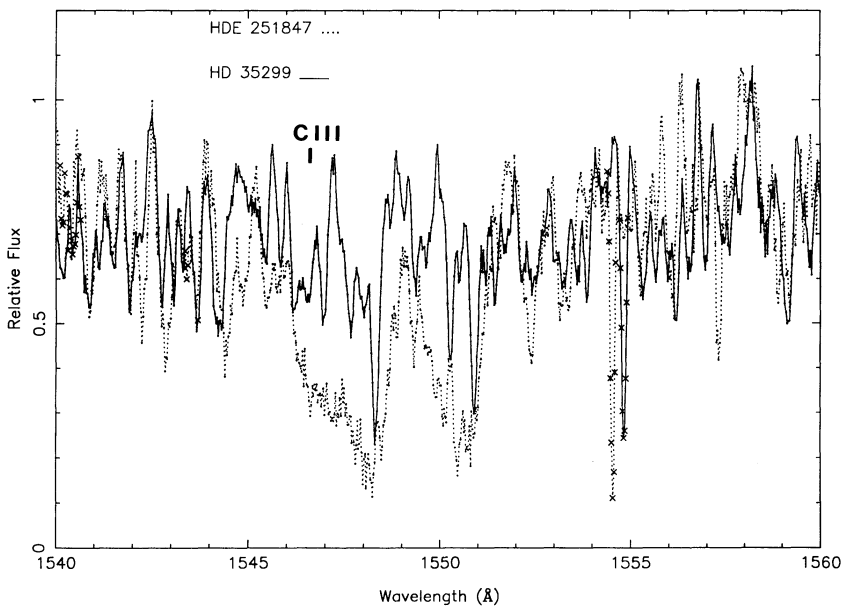

FIG. 5*b*

FIG. 5.—Comparison of the C IV region in HD 35299 ($T_{\rm eff}$ = 24,000 K, log g = 4.0) with HD 34816 and HD 66665 (both with $T_{\rm eff}$ = 28,000 K, log g = 4.0). The iron lines show little dependence on temperature, but the C IV lines respond strongly to the temperature increase.

that ambiguity into account in the estimates of the uncertainties of the intersection points.

These hand-drawn points are input interactively (using software written by J. A. G.) and displayed on a Sun workstation running PGPLOT (Pearson 1990). The dashed line is a result of interpolation between the two points, with typically 10 evenly spaced interpolations per interval. The software automatically measures the parameters in equation (1) from the input profile and computes the wind parameter. Also computed is the equivalent width of the input profile. The hand-drawn profile is intended to be a measure of total carbon absorption: included are contributions due to shortward-shifted discrete absorption components (DACs) caused by C IV, but contributions from weak photospheric iron lines that blanket this part of the spectrum are excluded. Like the extrapolation of profiles described above, this is a procedure that involves some ambiguity. In the slowly rotating stars it is fairly straightforward to distinguish the carbon absorption from the iron blends (see above), because of the velocity separation of the discrete C IV components. These stars may be used to make the same identification in the more rapid rotators. Since we considered the DACs to be part of the total carbon

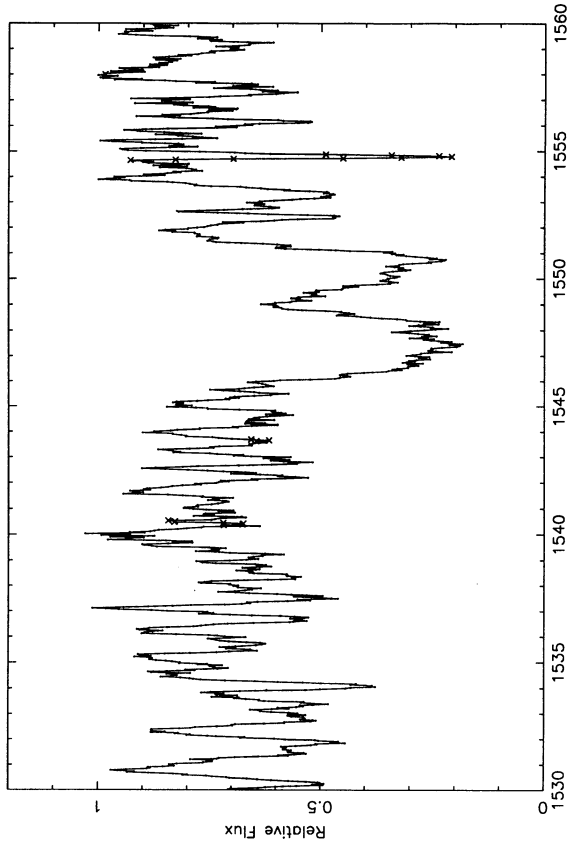

FIG. 6b

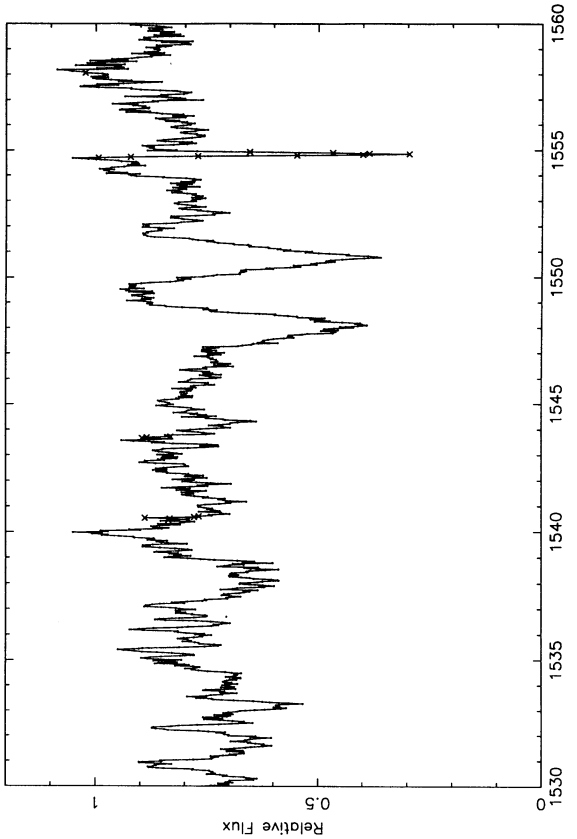

FIG. 6a

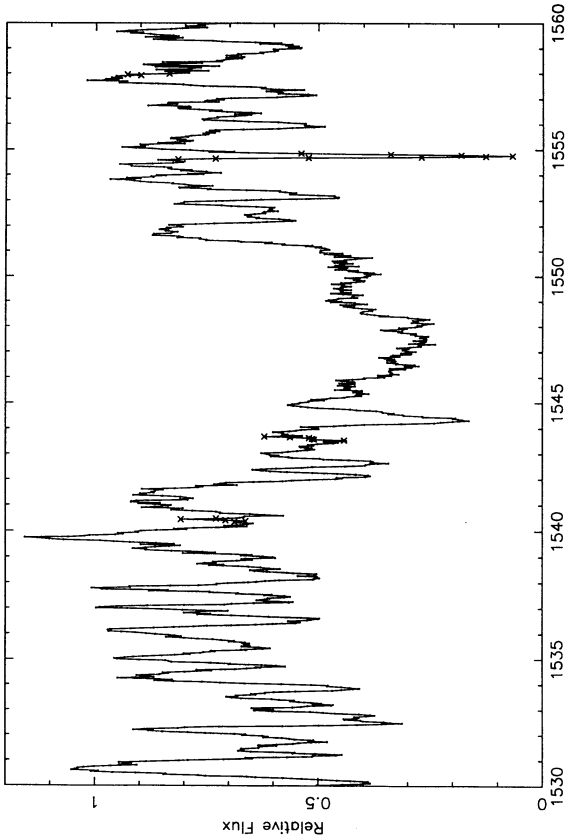

FIG. 6c

FIG. 6.—Progression of the C IV profiles with effective temperature in three stars, all with log $g = 4.0$. (*a*) A star with no asymmetry, (*b*) an incipient wind, and (*c*) a well-developed wind. Values of $v \sin i$ follow HD numbers, in parentheses, in units of km s^{-1}: HD 21856 (100), HD 34816 (30), and HD 218342 (30).

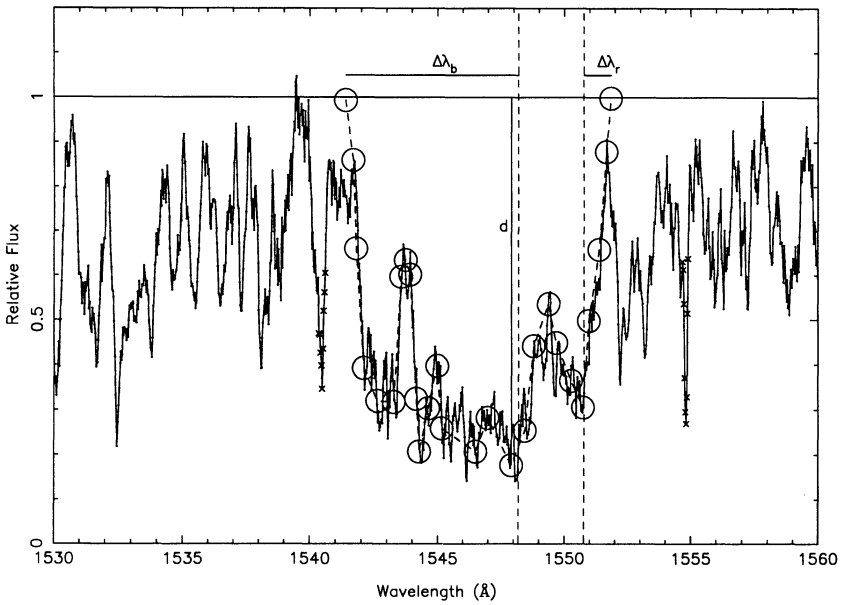

FIG. 7.—Example of a hand-drawn profile for HD 207538 used to compute the wind profile. Circles denote the location of points chosen by the user, and the profile used to determine the equivalent width is delineated by the dashed line. The dashed vertical lines indicate the rest wavelengths of the C IV doublet. The horizontal line shows the location of the continuum. The solid vertical line indicates the depth parameter d, and its wavelength represents the wavelength of maximum depth.

absorption, in stars in which the DAC is the deepest part of the profile (e.g., HD 35653) the DAC depth is taken as the depth parameter d.

Nevertheless, it is difficult to separate the effects of Fe and C IV absorption in many cases. In the example shown in Figure 7, the feature that is identified in the longward part of the hand-drawn profile as due to carbon may indeed be an iron blend. Such misidentifications have no effect on the value of the wind parameter, but will affect the equivalent width measurement. We attempt to account for possible misidentification of wind features with a large estimate of the equivalent width uncertainty.

Table 2 shows P_w and total C IV equivalent width in the program stars, along with the measured quantities $\Delta\lambda_b$, $\Delta\lambda_r$, and d and their estimated uncertainties. The error in P_w is due to uncertainties in continuum placement and in the measured quantities from which it is calculated; since we are fairly confident of continuum placement, we take the latter to be the dominant contributor, and the uncertainty in P_w is the sum of the errors, in quadrature, of the errors in $\Delta\lambda_b$, $\Delta\lambda_r$, and d. The uncertainty in equivalent width is more difficult to quantify and is prone to systematic error as discussed above if photospheric blends are misidentified as C IV wind features. The uncertainties are estimates based on the scatter resulting from numerous measurements of several spectra.

5.3. *Temperature and Luminosity Dependence of P_w and* C IV *Equivalent Width*

Figure 8 displays the temperature dependence of P_w. The stars with log $g \cong 4$ show a clear monotonic increase in P_w with effective temperature. If the asymmetry of the C IV lines is an accurate indication of stellar winds, then mass loss begins at effective temperatures of 26,000–27,000 K for a surface gravity of 4 dex, where values of P_w become significantly greater than zero. Certainly at 28,000 K, the doublet is unquestionably asymmetric, but at 25,000 K and below it appears photospheric (where it appears at all), possessing neither an asymmetry nor a radial velocity displacement relative to other photospheric lines. DACs do not play a significant role in the identification of the critical temperature and gravity where asymmetries first appear, simply because none of the stars near that region of the H-R diagram display them. The stars that do exhibit DACs generally are hotter than 28,000 K or display log $g < 4.0$ (e.g., HD 35653, HD 152246, HD 163892, and HD 218195). As a consequence of the symmetry of the doublet in the stars with effective temperatures at or below 25,000 K, P_w is consistent with zero in those stars and they display no evidence of mass loss.

Two stars with a similar surface gravity that do not agree with this picture are the OBCN stars HD 12323 and HD 201345 ($T_{\rm eff}$ = 29,000 K). Both display weak carbon lines for their effective temperature. A possible explanation is that these stars are carbon underabundant (Walborn 1976), consistent with the results of Paper I, where we found the optical carbon lines in these stars to be weak with respect to those in stars with similar effective temperatures. HD 12323 shows very weak C IV with no trace of asymmetry, while HD 201345 exhibits a stronger line and only the beginnings of asymmetry. The fact that these stars do not display evidence for a wind in the carbon lines does not necessarily indicate that they do not lose mass. As shown in Figure 2, the N V resonance lines ($\lambda\lambda$1239, 1243) in HD 12323 appear blueshifted (Walborn et al. 1985), and in HD 201345 the same lines are blueshifted and possibly asymmetric.

The other stars that do not lie near the log $g = 4$ locus possess significantly lower gravities. This effect is particularly apparent in the star HD 35653. At an effective temperature of 25,000 K, it displays a strong asymmetry in C IV, with obvious narrow, shortward-shifted DACs. Stronger wind signatures in lower gravity stars are expected because of the lower escape velocity and the shift of the carbon ionization balance toward higher stages of ionization in the photospheres of such stars

TABLE 2

C IV WIND PARAMETERS AND EQUIVALENT WIDTHS

Star (HD/HDE)	$\Delta\lambda_b$ (Å)	$\delta\Delta\lambda_b$ (Å)	$\Delta\lambda_r$ (Å)	$\delta\Delta\lambda_r$ (Å)	d[a]	λ_d[b] (Å)	P_w (Å)	δP_w (Å)	W (Å)	δW (Å)
12323	1.3	0.5	0.5	0.5	0.68	1548.0	0.5	0.7	1.5	0.8
13621	4.0	0.2	0.4	0.4	0.76	1547.7	2.7	0.5	3.8	0.8
21856	1.3	0.5	1.0	0.5	0.65	1550.7	0.2	0.3	1.5	0.8
24131	1.2	0.5	0.9	0.5	0.69	1548.0	0.2	0.3	1.7	0.8
34816	3.1	0.8	0.4	0.5	0.79	1547.6	2.1	0.7	3.4	0.8
35299	0.1	0.4	0.4	0.4	0.74	1548.2	−0.2	0.6	0.8	0.3
35653	7.0	1.0	0.8	0.4	0.82	1545.4	5.1	1.0	6.2	0.8
36430[c]	...	...	...	...	...	...	0.0	...	0.0	...
36822	6.4	1.0	1.2	0.5	0.75	1547.7	3.9	1.0	4.7	0.8
36824	2.9	0.4	0.8	0.4	0.37	1550.9	0.5	0.8	0.8	0.8
37209	0.9	0.3	0.8	0.3	0.65	1548.2	0.1	0.8	1.4	0.8
37366	6.3	0.4	0.5	0.4	0.70	1548.2	4.1	0.6	4.4	0.8
66665	4.1	0.4	1.6	0.4	0.98	1548.1	2.5	0.8	5.8	0.8
120307.....	0.8	0.4	0.9	0.4	0.52	1550.8	−0.1	0.3	0.9	0.8
132058.....	1.1	0.4	0.6	0.4	0.65	1547.9	0.3	0.4	1.2	0.8
142669.....	1.1	0.3	0.4	0.3	0.39	1547.8	0.3	0.3	0.7	0.8
143275.....	3.3	1.0	0.5	0.4	0.65	1547.5	1.9	0.9	2.9	0.8
144470.....	0.9	0.5	0.8	0.5	0.50	1550.7	0.1	0.5	1.3	0.8
148703.....	1.1	0.4	0.6	0.4	0.53	1548.2	0.3	0.5	1.1	0.8
149438.....	6.5	0.6	1.7	0.4	0.85	1547.5	4.1	0.8	5.8	0.8
151985.....	1.0	0.4	0.9	0.4	0.51	1548.2	0.1	0.5	1.1	0.8
152246.....	13.9	1.0	0.9	0.5	0.87	1542.1	11.3	1.3	10.7	0.8
163892.....	8.5	0.8	0.7	0.5	0.87	1540.9	6.8	1.1	7.9	0.8
201345.....	2.9	0.5	0.7	0.5	0.78	1550.0	1.7	0.7	3.7	0.8
207538.....	6.6	0.5	0.6	0.5	0.77	1546.4	4.6	0.7	6.2	0.8
208440.....	1.2	0.5	0.6	0.5	0.63	1550.4	0.4	0.6	1.6	0.8
214680.....	6.8	0.5	0.9	0.5	0.78	1546.3	4.7	0.8	6.2	0.8
217101.....	1.3	0.5	0.8	0.5	0.45	1550.5	0.2	0.4	1.0	0.8
218195.....	12.7	1.2	−0.2	0.8	0.96	1536.9	12.4	1.9	10.0	0.8
218342.....	7.0	0.5	0.8	0.5	0.73	1547.3	4.5	0.7	5.4	0.8
251847.....	3.2	0.5	0.8	0.5	0.81	1548.0	1.9	0.7	3.7	0.8

[a] Uncertainty in d: 0.05 in continuum units.
[b] λ_d = wavelength of maximum profile depth.
[c] Line probably not present.

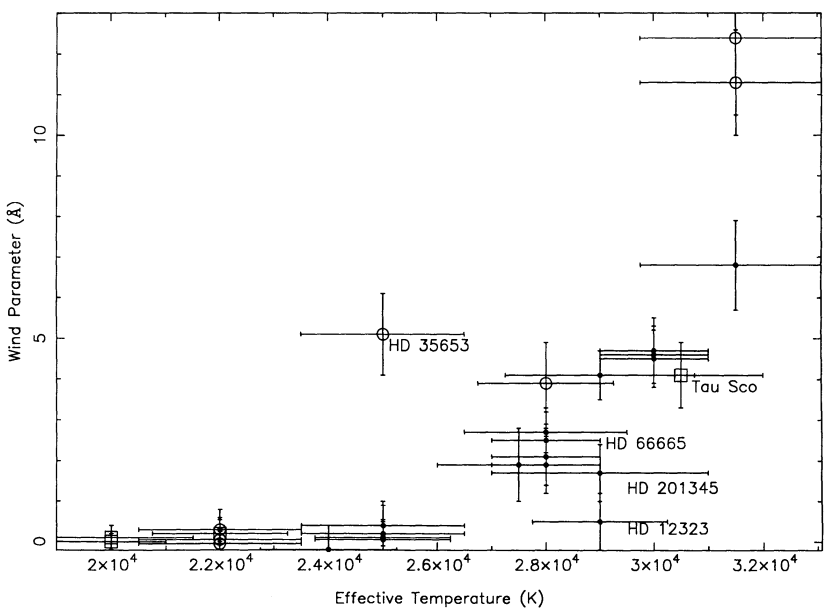

FIG. 8.—Dependence of the wind parameter on effective temperature. Stars that are labeled are discussed further in the text. The symbols are the same as in Fig. 1.

(Paper I). It is clear from Figure 8 that the temperature where asymmetries become measurable for stars of lower gravity is between 22,000 and 25,000 K, but with our limited data on such stars we are unable to constrain "turn-on" temperatures further.

Another interesting aspect of Figure 8 is the position of the "enhanced wind" star (Walborn et al. 1985) τ Sco (HD 149438). Its position in that figure does not imply that its wind is enhanced for its effective temperature; on the contrary, compared to stars with effective temperatures near 30,000 K, its P_w is somewhat smaller. However, τ Sco does possess a significantly larger surface gravity than those stars. If it were compared to stars of its gravity, its wind might still turn out to be enhanced.

In spite of having nearly the same value of P_w as the three stars at 30,000 K, τ Sco has a C IV profile that is markedly different: much less asymmetric and less shifted to shorter wavelengths, but significantly deeper (see Fig. 9*a*). In view of the strength of this star's UV resonance lines, it is interesting that Waters et al. (1993) have tentatively identified this star as a pole-on Be star based upon emission in certain hydrogen Brackett lines. This connection should be investigated further.

Like τ Sco, HD 66665 has a nearly normal value of P_w but unusually symmetrical, deep C IV resonance lines. In fact, these

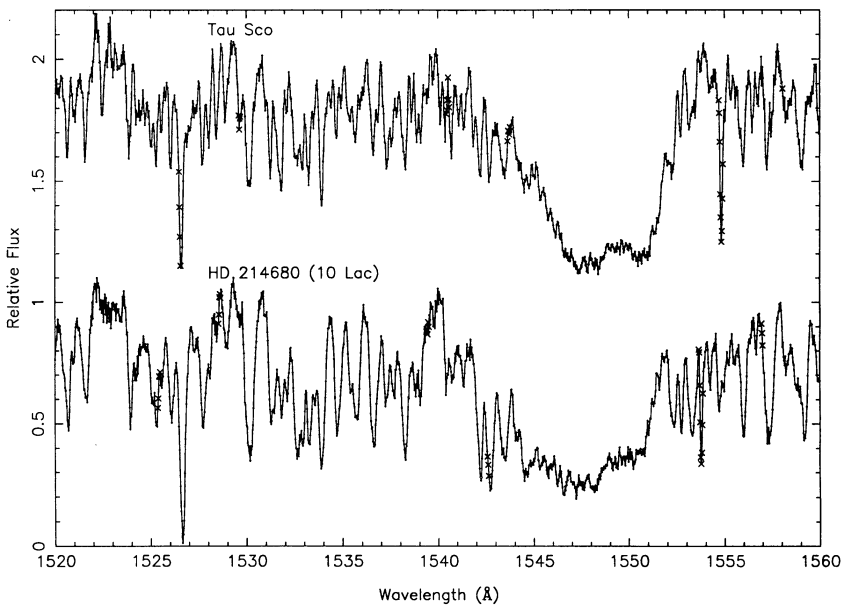

FIG. 9*a*

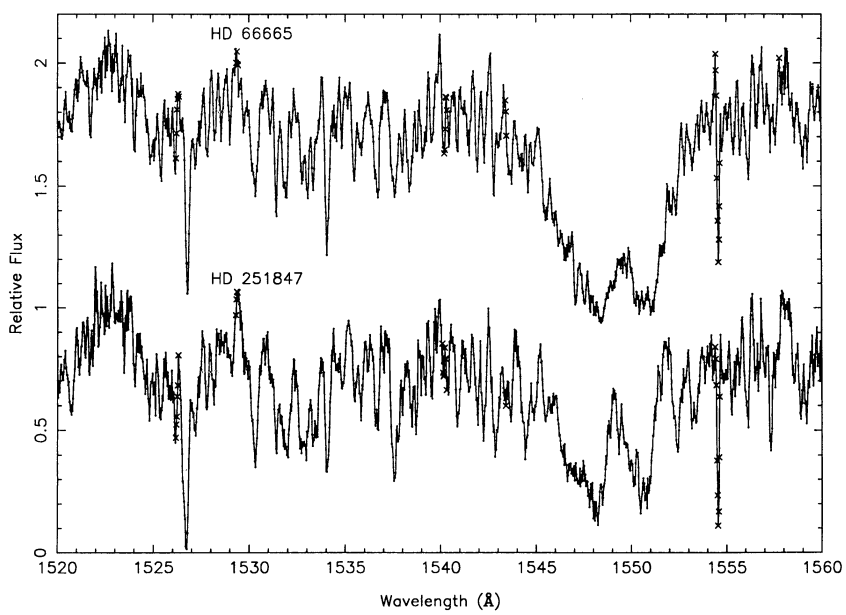

FIG. 9*b*

FIG. 9.—Comparison of the C IV profiles in selected stars. Note the similarity in the profiles of τ Sco ($T_{\rm eff}$ = 31,500 K, log g = 4.25) and HD 66665 ($T_{\rm eff}$ = 28,000 K, log g = 4.0). The profile of 10 Lac ($T_{\rm eff}$ = 30,000 K, log g = 4.0) is markedly different from that of τ Sco.

lines greatly resemble those of τ Sco, with the exception that they appear even more photospheric and deeper (Figs. 9*a* and 9*b*). This star has a projected rotational velocity that is among the smallest in the sample and possesses by far the strongest photospheric C IV resonance lines of any star in the program; as previously noted, other UV resonance lines are also unusually strong (Grigsby 1992). Because of this star's similarity to τ Sco, observations of its H Brackett lines would be of great interest.

Figure 10 shows the temperature dependence of C IV equivalent width as measured by the hand-drawn profiles. Superimposed upon this figure are synthetic photospheric C IV equivalent widths produced by PAM (Paper I). The similarity between the trends of P_w and equivalent width with temperature suggests that P_w is related to overall carbon absorption. The one point that is clearly different is that representing HD 66665. The great strength of the C IV doublet in this star is clearly shown in Figure 10.

The dependences of the wind parameter and C IV equivalent width on luminosity are shown in Figures 11*a* and 11*b*; we offer these plots as observational results. Both P_w and equivalent width show a strong correlation with luminosity. An attempted eyeball fit of a straight line to the data in Figure 11*a* suggests that there is a sudden drop in P_w at a luminosity somewhere between 4.2 and 4.5 dex. Clearly, the C IV doublet does not show evidence of winds for $\log (L/L_\odot) < 4.0$.

The apparent horizontal clustering of the data points may not be significant, given the size of the error bars: the maximum scatter is about 2 σ. It has been suggested (see the review by Bedding 1993) that δ Sco (HD 143275) has an anomalously low mass-loss rate for its luminosity. In Figure 11*a*, however, it is not at all unusual. It does lie below the main trend in Figure 11*b*, but HDE 251847 lies very close to it in that figure. For both stars, the lower extension of the error bar in luminosity would place them in the zone where P_w drops steeply to zero. In short, both are probably transition objects. Much more clearly anomlalous for its luminosity is HD 13621. This star, is, however, normal for its temperature and gravity. In view of its unusually high luminosity for its temperature and gravity (Fig. 1), perhaps the luminosity is the source of the anomaly. The possibility that this star may have an undiscovered, equally luminous companion seems unlikely because our model atmospheres match the optical spectrum unusually well (Paper I). Perhaps HD 13621 lies closer to us than the association.

Our sample has seven stars in common with those of Howarth & Prinja (1989) and Prinja (1989), who used line-profile fitting to determine the product of the mass-loss rate and the ionization fraction of C^{+3}. Figure 12 shows a tight correlation between this quantity and P_w. This result supports our conclusion that P_w is a good stellar wind indicator for chemically normal stars. Both our Figure 11*a* and Figure 8 from Prinja (1989) are consistent with the hypothesis that mass loss "turns on" suddenly in main-sequence stars at $\log (L/L_\odot) \sim 4.5$ and strengthens steeply with increasing luminosity above that value. Of course, the steep slope just above the threshold could be caused by a rapid increase in the ionization fraction of C^{+3}, and the slope of $\log \dot{M}$ itself could be a constant.

6. COMPARISON WITH STATIC, NON-LTE MODEL PHOTOSPHERES

Figure 8 shows that, in near–main-sequence stars, the C IV absorption lines acquire their asymmetry and cease to be purely photospheric in origin at effective temperatures between 25,000 and 27,000 K. Although we did not compute model stellar winds, we attempted to gain insight into the cause of asymmetrical C IV absorption by studying the physical conditions related to C IV line formation in our model photospheres. The good agreement between the synthetic and the observed C IV equivalent widths at $T_{\rm eff} = 25{,}000$ K (§ 5 and Fig. 10) suggests that PAM simulates these conditions realistically.

The temperature structure of two models is shown in Figure 13, and the figure also illustrates the relationship between

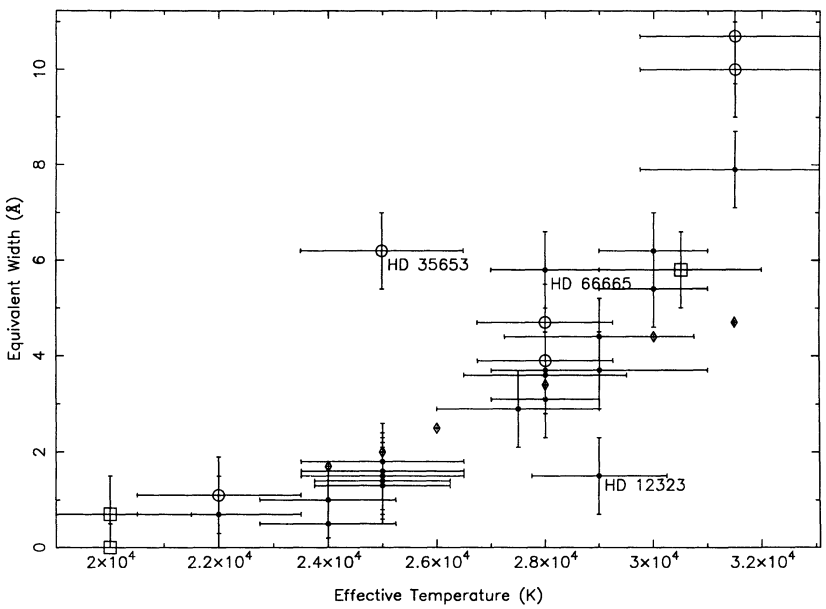

FIG. 10.—Temperature dependence of C IV equivalent width in the program stars. Diamonds represent model photospheric equivalent widths as predicted by the calculations of Paper I. Other symbols are as in Fig. 1.

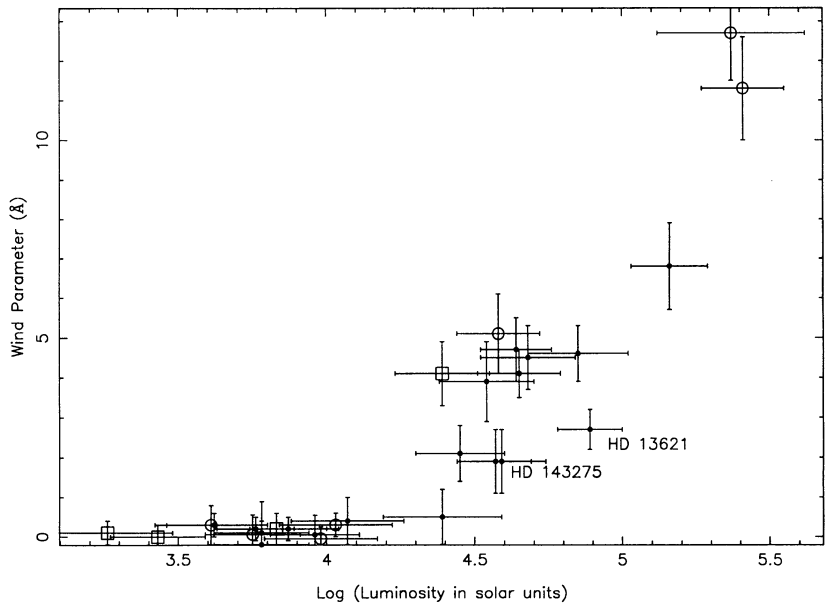

FIG. 11*a*

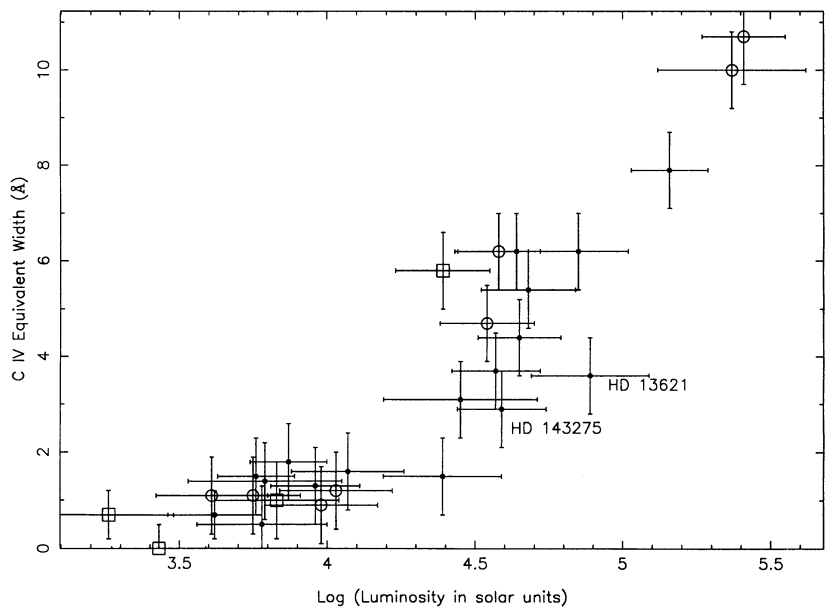

FIG. 11*b*

FIG. 11.—Dependence of (*a*) wind parameter and (*b*) C IV equivalent width as a function of luminosity (in solar units)

column density and level number. The continuum emerges from roughly level 40, a region several thousand degrees hotter than the line-forming region. Figure 14 shows the PAM predictions of the populations of the ground state of C IV (relative to all other carbon atomic states; the sum of the populations of all carbon states is unity) as a function of effective temperature for five levels in the model atmosphere. Strikingly, at effective temperatures above 27,000 K, the C IV ground-state population is larger at level 1 than at level 40. *This is a completely non-LTE result*! At 31,500 K the population of level 10 also exceeds that of level 40. The populations at levels 20 and 30 are depressed relative to those at level 40 in all models; these populations are typically smaller than those at level 1 by an order of magnitude or more. The model also indicates that the line core optical depth of the shortward component has not begun to approach unity in level 1 at an effective temperature of 25,000 K, but it is roughly unity in level 1 at 28,000 K, and at an effective temperature of 30,000 K it is 16.

7. DISCUSSION

These model predictions thus indicate that, at about ~28,000 K, the C IV line cores become optically thick at the top of the photosphere while remaining optically thin in the intermediate layers between the top and the level of continuum formation. Therefore, it is tempting to hypothesize that radiation pressure on C IV actually begins to drive the wind at this

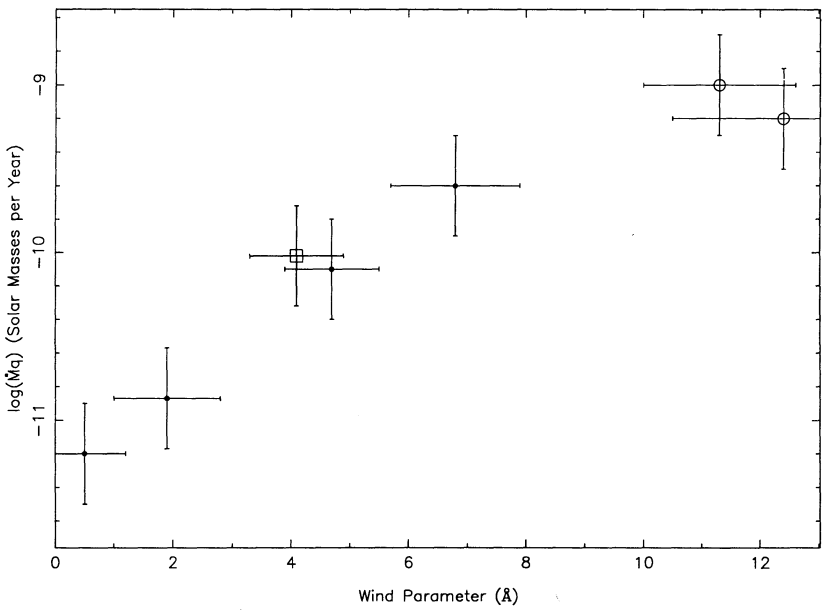

FIG. 12.—Correlation of the product of the mass-loss rate and C^{+3} ionization fraction (Howarth & Prinja 1989; Prinja 1989) with P_w, in the seven stars they had in common with the present work.

temperature. Both the opacity enhancement at the top of the photosphere and the relative transparency below should contribute to radiation pressure on C IV at the top of the photosphere, which could lead to the establishment of a wind.

Of course, radiation pressure on C IV ions does not explain cases like HD 12323, which shows a wind signature in the N V lines but not in C IV. In such C-poor stars, perhaps the N V lines play a similar role in initiating observable mass loss at a similar temperature. A full explanation of this effect should include line transfer in a moving atmosphere, preferably by means of a unified model atmosphere.

The alternative, more conventional, explanation for the transition from symmetrical to asymmetric C IV line profiles is that radiation-driven winds exist at temperatures and luminosities below this transition but are unobservable because the optical depth in the wind in the C IV doublet is too small. The transition from unobservability to observability would then be caused by an increase in the line core opacity of the outermost, moving layers of the atmosphere. The non-LTE population increase at the top of the photosphere, described above, could also explain such an opacity effect if it continued outward into the wind.

Therefore, our model photospheres are not capable of discriminating between these two hypotheses. In the following paragraphs, we will consider other arguments.

It is not implausible that the C IV resonance doublet could

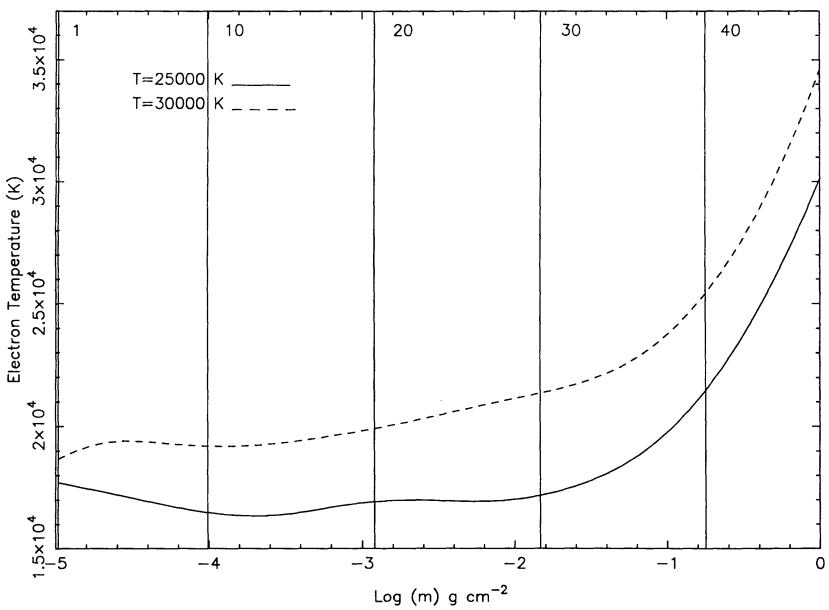

FIG. 13.—Electron temperature as a function of column density in two PAM models. The solid vertical lines illustrate the relationship between model level and column density.

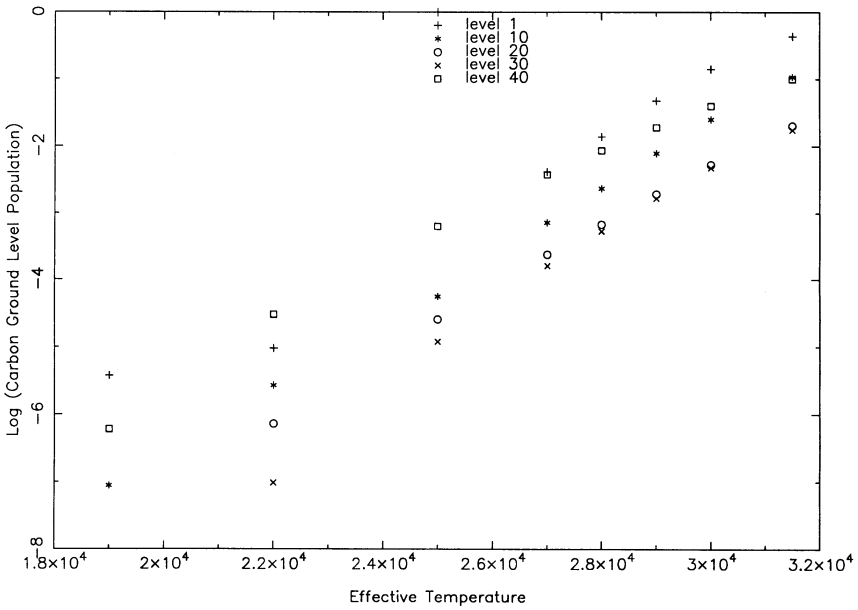

FIG. 14.—Model prediction for the relative population of the C IV ground state as a function of effective temperature. The point representing level 1 at $T_{\rm eff}$ = 25,000 K was unavailable and is missing. The ground-state population at level 1 (top of photosphere) exceeds that of level 40 at temperatures higher than 27,000 K.

be an important wind driver since it is the strongest unsaturated line near the peak of the energy distribution at this effective temperature. In the temperature regime under study, C, N, and O contribute more of the line acceleration than any other group of elements (Abbott 1982). When the wind is weak (small optical depth), the strongest lines are barely desaturated, and those lines dominate the radiation force. This situation, briefly mentioned in Abbott (1982), applies here.

Another argument in favor of the hypothesis that radiation-driven mass loss occurs only where it is actually observed in the C IV asymmetry is the general agreement between the location on the main sequence where winds appear and the location in the H-R diagram of the "static limit" computed by Abbott (1979) on the basis of radiation-driven wind theory. The static limit is the locus of points in the H-R diagram at which the line acceleration is equal to the effective acceleration of gravity. Above this locus, static atmospheres cannot exist and radiation-driven winds are inevitable. Below the locus, radiation pressure can sustain a wind if another mechanism sets up a velocity gradient in the atmosphere. Therefore, one expects the static limit to correspond, not necessarily to a boundary in the H-R diagram where winds disappear completely, but at least to a boundary where the incidence of stellar wind drops. Various authors, such as Abbott (1985b), have pointed out the general agreement between the theoretical static limit and the observational lower luminosity limit for observation of winds in ultraviolet resonance lines in normal stars.

On the other hand, the relevance of the static limit can be questioned. Perhaps many or all early B-type stars, by means of rapid rotation or pulsation, set up enough of a velocity gradient for radiation pressure to sustain a wind. In addition, the precise location of the static limit is not well determined by existing theory. Abbott's (1979) pioneering calcuation made several approximations, one of which is that the star is a point source as seen from the wind. More recent calculations have removed this approximation by incorporating the finite disk correction. According to Friend & Abbott (1986), the effect of that correction is to decrease the line acceleration at the base of the wind by a factor that can be as large as 0.6. With a decrease by this factor, we estimate that the static limit would move up in the H-R diagram by about $\Delta \log L = 0.2$. Although this change would improve agreement with our observed limit, caution is in order because the magnitude of this shift is comparable to observational error and because other approximations in Abbott's theory still need to be removed. For this reason, a detailed comparison between the static limit as calculated by Abbott (1979) and the boundary of the domain of observability of C IV profile asymmetry found in this study would be premature. It would be of great interest for the theoretical static limit to be recalculated by more rigorous methods (Kudritzki et al. 1989).

Perhaps the most sensitive diagnostic of a radiation-driven wind is emission of X-rays, which are believed to originate in shocks caused by instabilities in the wind. According to currently available evidence, X-ray emission persists to lower $T_{\rm eff}$ on the main sequence than does C IV profile asymmetry. For example, Cassinelli et al. (1994) found that main-sequence stars as low in effective temperature as 14,000 K show definite X-ray emission. On its face, this result is strong evidence that the threshold in C IV profile asymmetry is not a real wind threshold but only an optical depth effect.

But a confusing factor in the statistics of X-ray emission in hot stars is that binaries with companions of unknown spectral type are present in the sample. Coronal X-ray emission from a late-type companion would account for the observed flux of X-rays from mid-B-type stars in binaries (Meurs et al. 1992). In the sample of Cassinelli et al. (1994), only one of the three coolest stars detected (14,400–18,000 K) is not a binary with a companion of unknown type. Still, that sample, though admittedly small and heterogeneous, includes several apparently single, X-ray–emitting stars that are cooler than 26,000 K, and it is difficult to explain all of them away.

X-rays in a larger sample of early B-type stars were studied

by Meurs et al. (1992). In their Figure 3 is presented a histogram of the fraction of stars in which X-rays were detected with *ROSAT* as a function of spectral type. The fraction decreases strongly toward later type until it reaches a background level at which, on average, $\sim 10\%$ of the stars in each spectral class were detected. Although other explanations are possible, it may be that these background detections are binary systems that include coronally emitting, late-type components. Whatever its origin, this background is probably not caused by normal, radiation-driven winds. The latest spectral type at which the X-ray detection rate is more than 1 σ above this background is B1; a 2 σ criterion would place the threshold at B0. Therefore, it is not yet possible to rule out the hypothesis that the detectability threshold for radiation-driven winds in hot stars is at the same location in the H-R diagram for X-rays as it is for profile asymmetries in the C IV resonance doublet.

MacFarlane, Cohen, & Wang (1994) have shown that X-ray emission at the observed levels, if it originates in the stellar wind, significantly affects the ionization fractions in the winds and perhaps even in the photospheres of hot stars. At $T_{\rm eff} =$ 25,000 K, for example, they find an enhancement in the ionization fraction of C IV by at least four orders of magnitude in the wind (at $v = 0.5v_\infty$) compared to a model without X-rays, and they suggest that the X-ray emission results in a major enhancement of highly ionized species at the base of the wind also. In our non-LTE model photospheres, however, the computed and the observed C IV equivalent widths agree very well at and below an effective temperature of 28,000 K, without inclusion of X-rays or any other "superionization" mechanism. This result implies that X-rays are unimportant in the ionization balance of C IV in the photospheres of early B-type stars.

8. CONCLUSIONS

From our examination of the morphology of the C IV $\lambda\lambda$1548, 1550 resonance doublet, we conclude that the doublet is first detectably asymmetric in near–main-sequence stars (those with $\log g \cong 4 \pm 0.1$) of normal abundances at effective temperatures of 26,000–28,000 K and $\log (L/L_\odot) \cong 4.5$, when the model photospheric equivalent width of the C IV doublet is 2.4–3.0 Å. We find little evidence that iron or other weak photospheric blends mimic mass loss in marginal cases; the most straightforward explanation for the asymmetries is that they are caused by weak winds. The winds make their appearance at lower effective temperatures for stars of lower surface gravity, though with our limited data we cannot identify the threshold effective temperature in those stars. Some evidence for winds is seen in the N V and Si IV resonance doublets in some of the program stars of normal composition that possess evidence of winds, but the mass-loss signature is much stronger in the C IV doublet. We see little evidence for the existence of "enhanced mass loss" stars as described by other authors (e.g., Walborn et al. 1985), but stars such as τ Sco and HD 66665 do present unique C IV profiles and demand additional study. The problem of similarly classified stars with different C IV morphology that has been found by other workers appears partially solved, presumably because of the quantitative measurement of effective temperature and surface gravity in our program stars. Nevertheless, we still see cases in which stars with similar effective temperatures and surface gravities display markedly different C IV profiles (e.g., HD 13621, HD 34816, HD 66665, and HDE 251847 at an effective temperature of 28,000 K).

The initial appearance of the wind in this doublet coincides in effective temperature with a non-LTE effect: the population of the model C IV ground state is larger at the top of the photosphere than it is at the level of continuum formation for effective temperatures higher than 27,000 K; at intermediate photospheric levels, the population of the C IV ground state is an order of magnitude or more smaller than it is at the top of the photosphere. Non-LTE models also predict that the shortward component of the C IV doublet reaches optical depth unity at a column density of -5 dex. This combination of effects allows the underlying photosphere to exert a maximum radiative force on the top layers and may initiate mass motion in the photosphere. At 28,000 K the asymmetry in the doublet is measurable, and at higher temperatures the existence of a wind is evident through its asymmetry and blueshift. This scenario does not account for winds seen in the N V doublet in N-rich stars, which are carbon poor; that problem needs further investigation.

Section 7 of the paper concluded with a discussion of whether the boundary we have identified in the H-R diagram represented a real onset of radiation-driven winds or merely a threshold in the optical depth of the winds in the C IV resonance doublet. Neither the location of the theoretical "static limit" nor the incidence of X-ray emission in early B-type stars can yet be used to rule out the possibility that the threshold is real. Further work, both observational and theoretical, is needed to resolve this question.

We thank the staffs of the *IUE Observatory* and the Regional Data Analysis Facilities at Goddard Space Flight Center and at the University of Colorado in Boulder for help with the observations and the data analysis, respectively; we thank the National Space Science Data center for providing the archival data. We also thank Lawrence Anderson for his assistance with the modeling, Derck Massa for first drawing our attention to HD 66665, and Frank Feckel and Wayne Warren for helpful discussions about δ Sco. N. D. M. thanks the University of Toronto for hospitality during a sabbatical leave, and J. A. G. thanks the Wittenberg Faculty Development Organization for summer support and Nicole Jakopak and Mauricio Pedemonte for assistance with data reduction. Finally, we thank the referee for comments that led to significant improvements in this paper, especially § 7. This work was supported in part by NASA grant NAG 5-253, NASA SADAP grants NAG 5-970 and NAG 5-979, and made use of the database SIMBAD.

REFERENCES

Abbott, D. C. 1979, in IAU Symp. 83, Mass Loss and Evolution of O-Type Stars, ed. P. S. Conti & C. W. H. de Loore (Dordrecht: Reidel), 237
———. 1982, ApJ, 259, 282
———. 1985a, private communication
———. 1985b, in Relations Between Chromospheric-Coronal Heating and Mass Loss in Stars, ed. R. Stalio & J. B. Zirker (Italy: Tabographics-TS), 265
Anthony-Twarog, B. J. 1982, AJ, 87, 1213
Barbier, R., & Swings, J. P. 1979, A&A, 72, 374
Barker, P. K. 1984, AJ, 89, 899
Bedding, T. R. 1993, AJ, 106, 768
Bertiau, F. C. 1958, ApJ, 128, 523
Buser, R., & Kurucz, R. L. 1978, A&A, 70, 555
Cassinelli, J. P., Cohen, D. H., MacFarlane, J. J., Sanders, W. T., & Welsh, B. Y. 1994, ApJ, 421, 705

Castor, J. I., Abbott, D. C., & Klein, R. I. 1975, ApJ, 195, 157
Chavarria-K., C., de Lara, E., & Hasse, I. 1987, A&A, 171, 216
de Geus, E. J., de Zeeuw, P. T., & Lub, J. 1989, A&A, 216, 44
Friend, D. B., & Abbott, D. C. 1986, ApJ, 311, 701
Garmany, C. D., & Conti, P. S. 1984, ApJ, 284, 705
Garmany, C. D., Olson, G. L. Conti, P. S., & Van Steenburg, M. E. 1981, ApJ, 250, 660
Garmany, C. D., & Stencel, R. E. 1992, A&AS, 94, 211
Grady, C. A., Bjorkman, K. S., & Snow, T. P. 1987, ApJ, 320, 376
Grady, C. A., & Imhoff, C. L. 1985, IUE NASA Newsletter, No. 28, 86
Grigsby, J. A. 1991, ApJ, 380, 606
———. 1992, BAAS, 24, 800
Grigsby, J. A., Morrison, N. D., & Anderson, L. S., 1992, ApJS, 78, 205 (Paper I)
HIPPARCOS Input Catalog. 1992, Vol. 6, Annex 1, Double and Multiple Stars (ESA SP-1136) (Noordwijk: ESA Publications Division)
Howarth, I. D., & Prinja, R. K. 1989, ApJS, 69, 527
Hubeny, I., Stefle, S., & Harmanec, P. 1985a, Bull. Astron. Soc. Czechoslovakia, 36, 214
———. 1985b, Bull. Astron. Soc. Czechoslovakia, 37, 370
Humphreys, R. M. 1979, ApJS, 38, 309
IUE Regional Data Analysis Facility User's Tutorial Manual. 1990, Version 6.0, December 3
Johnson, H. L. 1966, ARA&A, 4, 9
Jones, D. H. P. 1971, MNRAS, 152, 231
Kimeswenger, S., & Weinberger, R. 1989, A&A, 209, 51
Kudritzki, R. P., Pauldrach, A., Puls, J., & Abbott, D. C. 1989, A&A, 219, 205
Kurucz, R. L. 1987, private communication
Lamers, H. J. G. L. M., & Groenewegen, M. A. T. 1990, in ASP Conf. Ser., 7, Properties of Hot Luminous Stars: Boulder-Munich Workshop, ed. C. D. Garmany (San Francisco: ASP), 189
Leckrone, D. S., & Adelman, S. J. 1989, ApJS, 71, 387
MacFarlane, J. J., & Cassinelli, J. P. 1989, ApJ, 347, 1090
MacFarlane, J. J., Cohen, D. H., & Wang, P. 1994, ApJ, 437, 351
Maeder, A., & Meynet, G. 1988, A&AS, 76, 411
Massa, D. 1985, private communication
McCall, M. L., Richer, M. G., & Visvanathan, N. 1990, ApJ, 357, 502
Meurs, E. J. A., et al. 1992, A&A, 265, L41
Murdin, P., & Penston, M. V. 1977, MNRAS, 181, 657
Olson, G. L. 1982, ApJ, 255, 267
Pauldrach, A. W. A., Puls, J., Gabler, R., & Gabler, A. 1990, in ASP Conf. Ser., 7, Properties of Hot Luminous Stars: Boulder-Munich Workshop, ed. C. Garmany (San Francisco: ASP), 171
Pearson, T. J. 1986, PGPLOT Graphics Subroutine Library (Pasadena: Caltech)
Perry, C. L., Hill, G., & Christodoulou, D. M. 1991, A&AS, 90, 195
Prinja, R. K. 1989, MNRAS, 241, 721
Prinja, R. K., Barlow, M. J., & Howarth, I. D. 1990, ApJ, 361, 607
Rountree, J., & Sonneborn, G. 1991, ApJ, 369, 515
Strom, S. E., Strom, K. M., & Carrasco, L. 1974, PASP, 86, 798
Turnrose, B. E., & Thompson, R. W. 1984, International Ultraviolet Explorer Image Processing Information Manual, Version 2.0 (New Software), CSC/TM-84/6058
Walborn, N. R. 1976, ApJ, 205, 419
Walborn, N. R., Nichols-Bohlin, J., & Panek, R. J. 1985, IUE Atlas of O-type Spectra from 1200 to 1900 Å (NASA RP-1155) (Greenbelt: NASA)
Walborn, N. R., & Planck, R. J. 1984, ApJ, 286, 718
Warren, W. H., Jr., & Hesser, J. E. 1978, ApJS, 36, 497
Waters, L. B. F. M., Marlborough, J. M. Geballe, T. R., Oosterbroek, T., & Zaal, P. 1993, A&A, 272, L9